

RESEARCH ARTICLE

Physicochemical analysis of Magnesium Oxide Nanoparticles via Mango Peel Extraction approach: cytotoxic impact on MCF7 cell line

Ameena Abdullah Rustum¹, Mais Emad Ahmed^{2*}, Adawia Fadhil Abbas¹

¹ Department of Biology, College of Education Pure Science, University of Diyala, Iraq

² Department of Biology, College of Science, University of Baghdad, Iraq

ARTICLE INFO

Article History:

Received 05 Jun 2025

Accepted 09 Aug 2025

Published 01 Sep 2025

Keywords:

Mg(NO₃)₂

X-ray diffraction (XRD)

Mango Peel

Breast cancer cell line

ABSTRACT

Objective(s): Sustainable bimetallic nanoparticles (NPs) have attracted a lot of attention in the past ten years. However, the environment and efficiency concerns are related to their synthesis and property optimization. Here, we describe the environmentally friendly synthesis of bimetallic MgONPs utilizing Mango Peel Extraction (MPE) and cytotoxic activities that show promise for anticancer potential against the MCF7 cell line

Methods: This work presents a green production of magnesium oxide nanoparticles (MgO NPs) using mango peel extract (MPE) as a stabilizing and reducing agent. The biosynthesized MgO NPs were comprehensively physicochemically characterized using techniques such as scanning electron microscopy (SEM), Fourier-transform infrared spectroscopy (FTIR), X-ray diffraction (XRD), and UV-Vis spectroscopy.

Results: Mango peel extract was used to successfully create magnesium oxide nanoparticles (MgO-NPs), as demonstrated by UV-Vis spectroscopy, which showed an absorption peak at about 362 nm. The majority of the nanoparticles were spherical, with diameters between 14 and 20 nm and a uniform dispersion, according to TEM and FESEM investigations. While FTIR analysis revealed the existence of -OH, C=O, and Mg-O functional groups, indicating efficient capping by bioactive chemicals from the extract, EDX spectra revealed magnesium and oxygen as the primary elements. With a GI²¹ value of roughly 11 µg/mL, cytotoxicity tests on the human breast cancer cell line MCF7 showed a dose-dependent decrease in cell viability. MgO-NPs caused 65.4% cytotoxicity at 25 µg/mL, along with significant morphological alterations like cell shrinkage and membrane integrity loss. These results indicate that MgO-NPs synthesized via mango peel extract possess significant anticancer potential.

Conclusions: The bimetallic MgONPs that were successfully biosynthesized using MPE had significant biological engineering potential. Metal oxide nanoparticle biosynthesis is a great substitute for chemical synthesis.

How to cite this article

Abdullah Rustum A., Emad Ahmed M., Fadhil Abbas A. Physicochemical analysis of Magnesium Oxide Nanoparticles via Mango Peel Extraction approach: cytotoxic impact on MCF7 cell line. *Nanomed Res J*, 2025; 10(3): 281-294. DOI: [10.22034/nmrj.2025.03.007](https://doi.org/10.22034/nmrj.2025.03.007)

INTRODUCTION

Targeting microbes with nanoparticles is a common substitute for antibiotics. Broad-spectrum antibacterial properties are exhibited by nanomaterials and nanostructures [1]. The green synthesis of nanoparticles, which uses extracts from microorganisms and plant parts like leaves,

fruits, and seeds as reducing and capping agents, is a great alternative to expensive physicochemical methods that use hazardous reagents and toxic organic solvents that endanger the environment and human health [2]. It seems imperative to implement all agricultural strategies to increase fruit and vegetable production globally in view of concerns about population growth. Moreover,

* Corresponding Author Email: mais.emad@sc.uobaghdad.edu.iq

more than 40% of the fruit's mass—including the peel, pulp, and seeds—is inedible, despite the fact that many fruit varieties—such as bananas, watermelon, papayas, mangoes, and pineapples—are valued for their flavor and nutritional value [3]. To improve the safety and dependability of the NP generation processes, these NPs are made using high-energy renewable materials in a clean, non-toxic, and environmentally responsible manner [4]. Because the precise media and growing conditions required for other biological entities do not need to be maintained, the development of plant-fabricated NPs can move more quickly. Because of their huge surface areas and ability to boost reactivity by generating reactive oxygen species, green pathway NPs frequently have strong catalytic capabilities that can increase toxicity in bacterial cells and malignancies [5]. This process not only demonstrates a sustainable and cost-effective technique of NP synthesis, but it also introduces MgO-NPs with exceptional antibacterial properties. At low concentrations, these NPs demonstrated great action against a variety of harmful bacteria, which was an impressive accomplishment. [6]. Compared to other methods (chemical and physical), magnesium nanoparticles have significant adsorption and microbiological properties because of their interactions with various protein molecular structures. MgO-NPs produced biologically are more economically feasible, easier to utilize, and better for the environment [7]. The majority of the aforementioned issues could be effectively resolved by using biomaterials such as microorganisms, algae, biopolymers, plant materials, or their derivatives in the bio- (green) synthesis of NPs, which offers a simple, inexpensive, eco-friendly, and controllable approach [8]. The trash from the mango fruit that is discarded after usage is called mango peels. These peels can be used to make an extract that contains a variety of phytochemicals and phenolic components, such as polyphenols, flavonoids, carotenoids, and vitamins. These materials are utilized as an inexpensive stabilizing and reducing agent while producing several types of metal nanoparticles (MNPs). The hydroxyl groups in these compounds, which are a part of different functional groups, either produce MNPs with different sizes and shapes or reduce the metal ions. Many research has prepared MNPs using mango peel extract (MPE), a source of bioactive compounds that trap and transform

metal ions into metal atoms [9]. Magnesium has a well-established pharmacological potential, and its Nano formulation is anticipated to offer significant therapeutic effects, particularly in the battle against cancer. In this study, we investigated the anticancer potential of biogenically generated magnesium oxide nanoparticles (MgO NPs) against the breast cancer cell line MCF-7 [10]. Thus, in this study, crude mango peel extract (MPE) was used to create MgONPs with unique anticancer characteristics. The comparison study comprised tests for biological activity evaluation, topography, and physiochemistry. These MNPs are easily obtainable from sources such as peel and precursor salts, which makes them appropriate catalysts for a range of organic processes, sensing, and the biomedical sector in the future.

MATERIALS AND METHODS

Green MgONPs Synthesis

Preparation of the Mango Peel Extract (MPE)

Mango peels (*Mangifera indica*) that were cultivated organically were hand harvested after being cleaned with double-distilled water (DW) and left to air dry for 62 hours at 44 ± 2 °C. The dried peels were mechanically ground into a powder (100 g, roughly 60 mesh size), then extracted using 1 L of 70% diluted ethanol, stirred at room temperature (RT; 25 ± 2 °C) at centrifugal force (110xg) to RPM (revolutions per minute), and filtered to remove any leftover plant debris. Mango peel extract (MPE) was vacuum-dried at 41 °C and then redissolved in DW to achieve a 10% concentration. [11] **Fig.1.**

Biosynthesis of MPE- Magnesium Oxide Nanoparticles (MgONPs)

This approach produced a final concentration of 2 mM by mixing 10 mL of aqueous mango peel extract with 90 mL of deionized water that included 51.3 mg of $\text{Mg}(\text{NO}_3)_2 \cdot 6\text{H}_2\text{O}$. After stirring the mixture for an hour at 40°C, 5 mL of 1 N NaOH was progressively added to raise the pH to 8. A brown precipitate of $\text{Mg}(\text{OH})_2$ that had formed after standing all night was calcined to create MgO nanoparticles (MgO-NPs). After gathering the precipitate and thoroughly cleaning it with deionized water to remove any contaminants, it was calcined at 200°C for four hours [16]. Control investigations employed plant extract devoid of the metal precursor and deionized water containing only $\text{Mg}(\text{NO}_3)_2 \cdot 6\text{H}_2\text{O}$. [12].

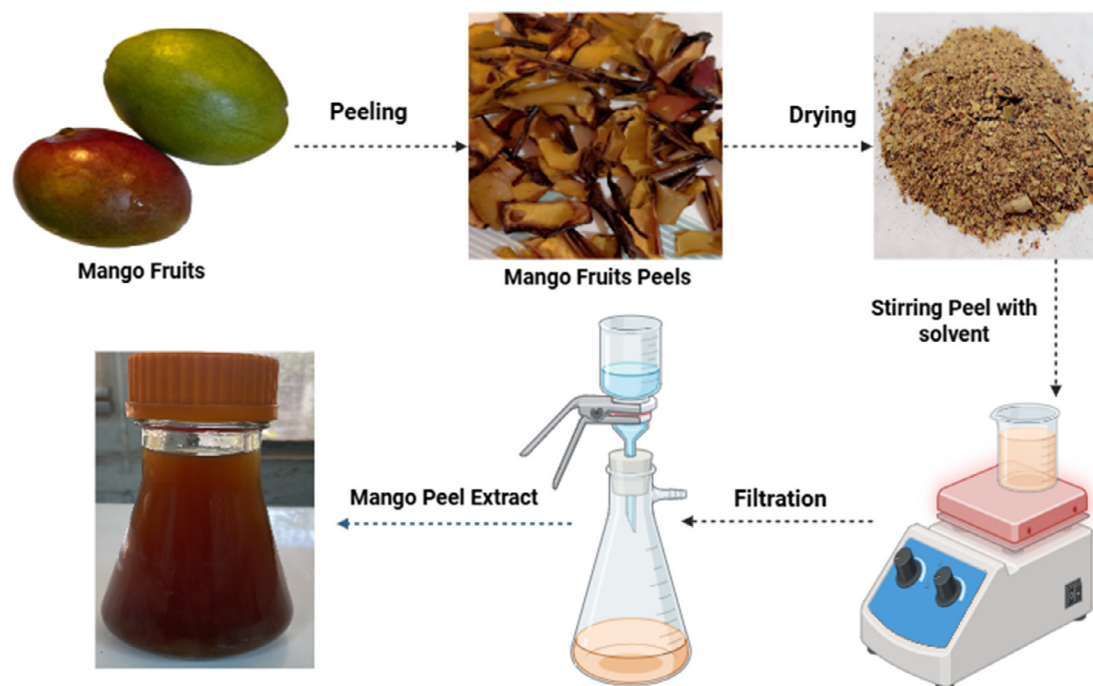


Fig. 1. MPE preparation

Particle size and surface charge

The DLS “dynamic light scattering” method was used to evaluate the Zeta (ζ) potentialities and particle size (Ps) of MPE-synthesized MgONPs and their mixed forms (MPE/MgO NPs) utilizing the Zeta plus.

Nanoparticles ultrastructure

The SEM (scanning electron microscope) was utilised to screen for ultrastructure, including particle dispersion and topography, using an accelerating voltage of 20 kV. The form, dispersion, and Ps of the MPE-synthesised MgONPs ultrastructure were further examined using TEM imaging.

Characterisation of Magnesium Oxide Nanoparticles (MgONPs)

Using a Bruker equipment (Bruker Co., Ettlingen, Germany) with a wavelength range of $400\text{--}4000\text{ cm}^{-1}$, Fourier-transform infrared spectroscopy (FTIR) investigation was carried out to identify the functional groups involved in the production of MgO nanoparticles (MgONP). Additional characterisation techniques included energy-dispersive X-ray spectroscopy (EDX), ultraviolet-visible (UV-Vis) spectroscopy, and

atomic force microscopy (AFM). The UV-Vis absorption spectra of the MgONPs in the $200\text{--}600\text{ nm}$ range were recorded using a UV-Vis spectrophotometer (UV/Vis-1800, Shimadzu, Kyoto, Japan). The size and morphology of the powdered MgONPs were examined at a resolution of 500 nm using the Hitachi S-3400N scanning electron microscope (SEMEDX analysis was used to determine the elemental composition of the nanoparticles both qualitatively and quantitatively. Every characterisation was done in the Department of Chemistry, College of Science, University of Baghdad. [13].

UV-Visible Spectroscopy (UV-Vis)

(Japan/Shimadzu) To verify the production of nanoparticles, plasmon resonance and bulk electron oscillations in the conduction band in response to electromagnetic waves are measured using UV-visible spectroscopy. It includes comprehensive details about the size, stability, aggregation, and structure of nanoparticles. Using a spectrophotometer, selenium nanoparticles in the $200\text{--}600\text{ nm}$ range can be created. By measuring the reaction mixture’s wavelength in the spectrophotometer’s UV-VIS spectrum, MgONPs were verified.

Atomic force microscopy AFM

The size and surface shape of MgONPs nanoparticles were measured using (UNICCO/USA). A few drops of prepared MgONPs were applied to a quartz glass plate, and the plate was let to cure at room temperature in the dark to create a thin coating. AFM was then used to scan the lowered glass plate.

Fourier Transform Infrared Spectroscopy (FTIR)

The presence of functional groups primarily involved in the bioreduction of MgONPs was verified using FT-IR spectroscopy. The produced MgONPs' chemical bonds were analysed using FTIR by scanning in the 400–4000 cm⁻¹ wavelength range.

Energy Dispersive X-ray Analysis (EDX)

(Bruker, Germany) The qualitative and quantitative states of elements that might be involved in the creation of nanoparticles can be determined using EDX analysis. EDX microanalysers were used to assess the element content in specific regions of the SEM sections. The interaction between the material and the X-ray excitation sources determines the high purity of confirmed selenium nanoparticles produced in these investigations.

Scanning/Transmission Electron Microscopy (SEM/TEM)

(Japan's Hitachi Ltd.) The images were captured using a Hitachi s-3400N scanning electron microscope (SEM) with a resolution of 500 nm and detectors with a secondary electron; the size and shape of MgONPs were examined using BSE semiconductors (quad-type); this method is used to gather comprehensive information about surface NPs. The average particle shape and diameter of the nanoparticles were described using this method. A tiny drop of the dried MgONPs solution sample was placed on a microscope slide and allowed to dry after being sonicated with distilled water. After that, a tiny layer of platinum was applied to the samples to make them conductive.

X-ray Diffraction (XRD)

(Shimadzu/Japan) The crystal structure of MgONPs was measured by XRD to investigate the shape and dimension of the MgONPs powder sample.

Cytotoxicity assay

The in vitro MTT assay [3-(4,5-dimethylthiazol-2-yl)-2,5-diphenyltetrazolium bromide] was used to assess the cytotoxicity of MgO nanoparticles (MgONPs). To ensure appropriate cell adhesion, MCF-7 cells (7,000 cells/well) were seeded into 96-well plates and incubated overnight. After incubation, the cells were treated three times with escalating concentrations of MgONPs (6.25–100 µg/mL). Following the 24-hour treatment period, each well received 20 µL of MTT solution (5 mg/mL; Shanghai Macklin Biochemical Co., Ltd.) after the medium was withdrawn. After that, the plates were incubated for three hours at 37°C in the dark. The formazan crystals in each well were dissolved in 50 µL of dimethyl sulfoxide (DMSO; Bio Basic Inc.). Before the absorbance measurement, the plate was gently shook for ten minutes [14]. Absorbance at 490 nm was measured using a microplate reader from the raw absorbance data, the proportion of live cells was calculated using the following equation Eq.1.

$$\text{Eq.1: Viability \%} = \frac{\text{A test} - \text{A blank}}{\text{A control} - \text{A blank}} \times 100$$

where "A" stands for absorption. The dose-response curve was created using GraphPad Prism software version 6 (Dotmatics), and the growth inhibitory concentration (IC50), a value that decreases viability by 50%, has been determined using the same curve. [15].

RESULTS

Synthesis of MgONPs

Several phytochemical studies were conducted on the mango peel extract solution to confirm the bioactive compounds and the functional groups responsible for the reduction and capping of MgO-NPs. Alkaloids, tannins, phenols, flavonoids, and terpenoids were detected by these tests. Prior to the biosynthesis of MgO-NPs, several parameters, such as pH levels, plant extract concentrations, and metal precursor concentrations, were primarily investigated in order to find the optimal conditions for the manufacture of MgO-NPs based on the intensity of color changes. display Fig. 2

The first indication that the MgONPs were being synthesized was when the solution's color progressively changed from pale yellow to a deep brownish-orange tint after 60 minutes. MPE has been used to biosynthesize a number of metal NPs.

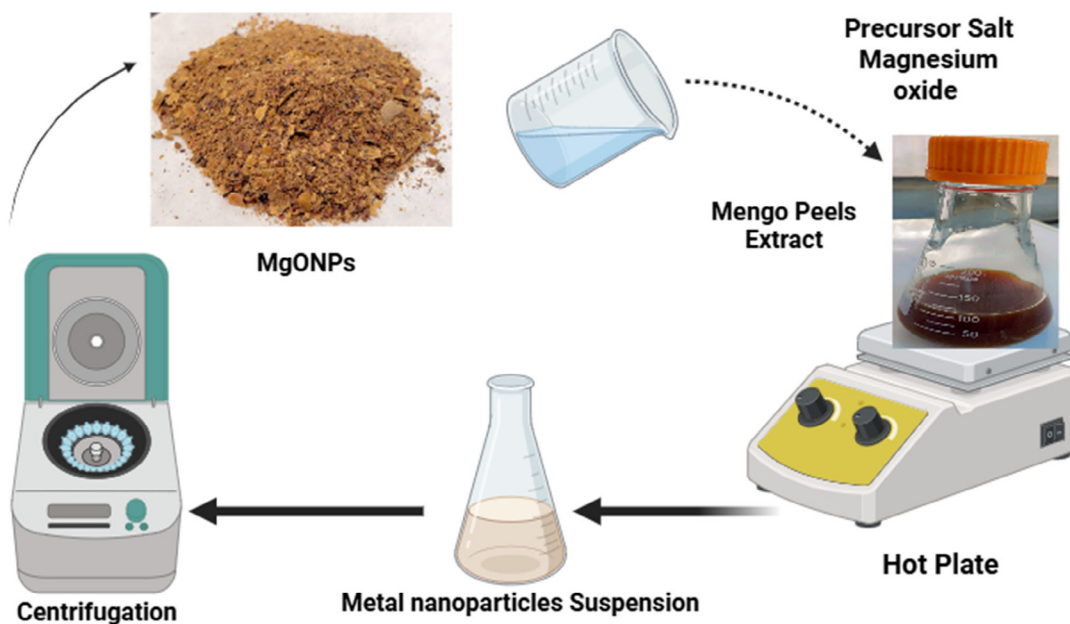


Fig. 2. Synthesis of MgONPs

Mango peel contains significant levels of phenolic chemicals, such as hydrolyzable tannins and flavonoids, which are necessary for the formation of metal nanoparticles. The weak red, white, and red colors that were observed, where MPE was acting as a capping or reducing agent, then suggested the biogenesis of MgONPs. Plant extracts contain bioactive phytochemicals that act as a capping agent, avoiding nanoparticle agglomeration and changing their biological activity.

Characterization of biosynthesized MgONPs UV-Visible (UV-VIS) spectroscopy

Since UV-Vis spectroscopy primarily provides information about the optical properties of nanoparticles, such as absorption peaks related to surface plasmon resonance, it was used to confirm the formation of the biosynthesized MgONPs rather than to examine their detailed morphological characteristics. A successful generation of the MPE is shown by an absorption peak at 250 nm, which corresponds to selenium from magnesium nitrate hexahydrate (Fig. 3a). While Fig. 3c displays an absorption peak at 283 nm, indicating the presence of individual MgONPs in the solution, Fig. 3b's peak at 362 nm verifies the production of nanoparticles. Particle size and shape cannot be directly measured by UV-Vis spectroscopy; instead, methods like

TEM or SEM should be used to ascertain these properties

Atomic force microscopy (AFM)

Atomic force microscopy has been used to measure the average diameter of MgONPs in addition to their two- and three-dimensional shape as a confirmatory technique to explain their biogenesis in general. The diameter of the synthesized MgONPs was 68 nm, according to the study's results, which are shown in Fig. 4.

FTIR analysis

The combined MPE/MgONPs spectrum analysis revealed the most responsible MPE groups for the biosynthesis of MgONPs. Figure 5. In the MPE/MgONPs spectra, however, the C-H band (at 2888 cm^{-1} in the MPE spectrum) mostly disappeared. 3434.89 cm^{-1} : This broad peak, which corresponds to O-H stretching vibrations, shows that the mango peel extract contains hydroxyl groups from leftover water or polyphenols. 2924.72 cm^{-1} —C-H stretching, which is typically linked to aliphatic $-\text{CH}_2$ or $-\text{CH}_3$ groups and is probably the result of organic molecules in the extract serving as capping agents. Proteins or polyphenolic chemicals from the extract may interact with MgONPs, as indicated by the C=O stretching of amide or

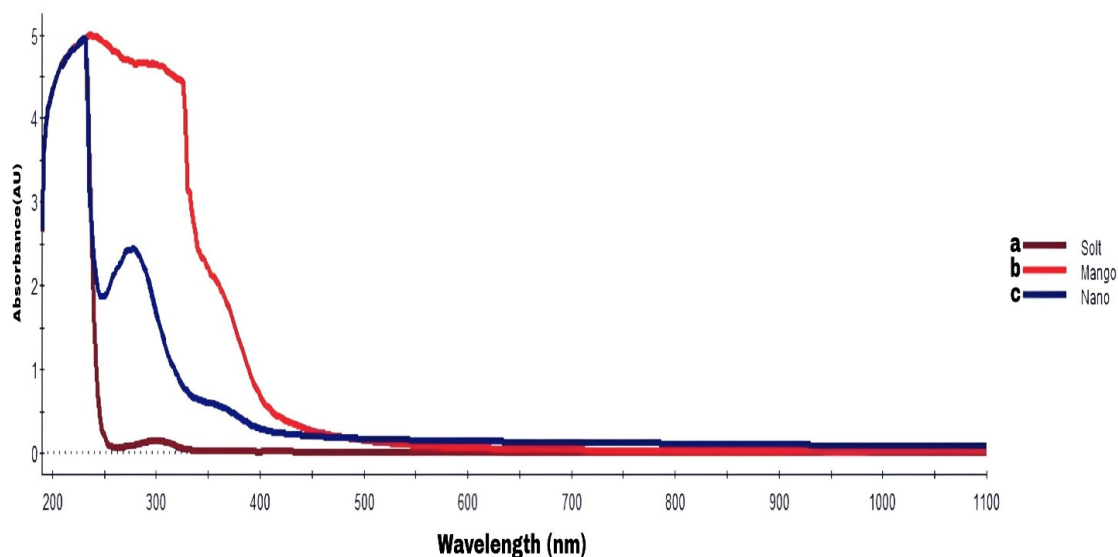


Fig. 3. UV--VIS spectroscopy analysis (a) Magnesium nitrate hexahydrate (b) mango peels extract (c) MgONPs

carbonyl groups at 1631.67 cm^{-1} . C–H bending of methyl or methylene groups is 1453.61 cm^{-1} . The symmetric bending of carboxylate ($-\text{COO}^-$) groups at 1376.64 cm^{-1} indicates that organic acids have stabilized the nanoparticles.

Polyphenols, carbohydrates, and proteins are responsible for the bands in the blank MPE spectrum that correspond to O–H, C=O, C–O, and C–H stretching. The majority of these organic bands are still visible in the MgONPs spectrum, suggesting that the extract's bioactive compounds are stabilising and capping the nanoparticles. The successful synthesis of magnesium oxide, which is not present in the blank extract, is confirmed by the emergence of Mg–O vibrations about 728 and 616 cm^{-1} in the MgONPs spectrum.

Energy dispersive X-ray (EDX)

The elemental composition of the MgONPs powder was ascertained by energy dispersive X-ray (EDX) spectroscopy (Table 1, Fig. 5). The effective synthesis of MgONPs was validated by the EDX spectra, which identified magnesium as the primary component. Both magnesium oxide and the capping/stabilizing agents made from the plant extract employed in synthesis may be responsible for the oxygen-corresponding peaks that were also found. There detected trace amounts of carbon, which are linked to the extract's phytochemicals. Furthermore, trace elements, including sodium and chloride, were found; these could be leftovers

from the extract's biomolecules or precursor salts. These findings are consistent with earlier reports showing that biologically synthesised nanoparticles often display additional elemental signals due to organic molecules serving as reducing and stabilizing agents

Field emission Scanning Electron Microscope (FESEM) and TEM

The biosynthesised MgONPs were mostly spherical and ranged in size from 10 to 60 nm , according to transmission electron microscopy (TEM) examination (Fig. 6a). Additionally, the TEM micrographs showed that the nanoparticles were distributed somewhat uniformly, suggesting excellent dispersion without noticeable agglomeration. The MgONPs' surface shape and particle size were further investigated using field emission scanning electron microscopy (FESEM) (Fig. 6b). The FESEM pictures demonstrated that the particles were uniformly shaped and almost spherical, which is in good agreement with the TEM results. The morphology of green-synthesised MgONPs is consistent with previous studies.

Zeta potential (ZP)

The biosynthesized MgONPs had an average particle size of 624.4 nm and a size distribution ranging from 75.5 to 4085.6 nm . This suggests a rather wide and polydisperse population of nanoparticles, which may be the consequence

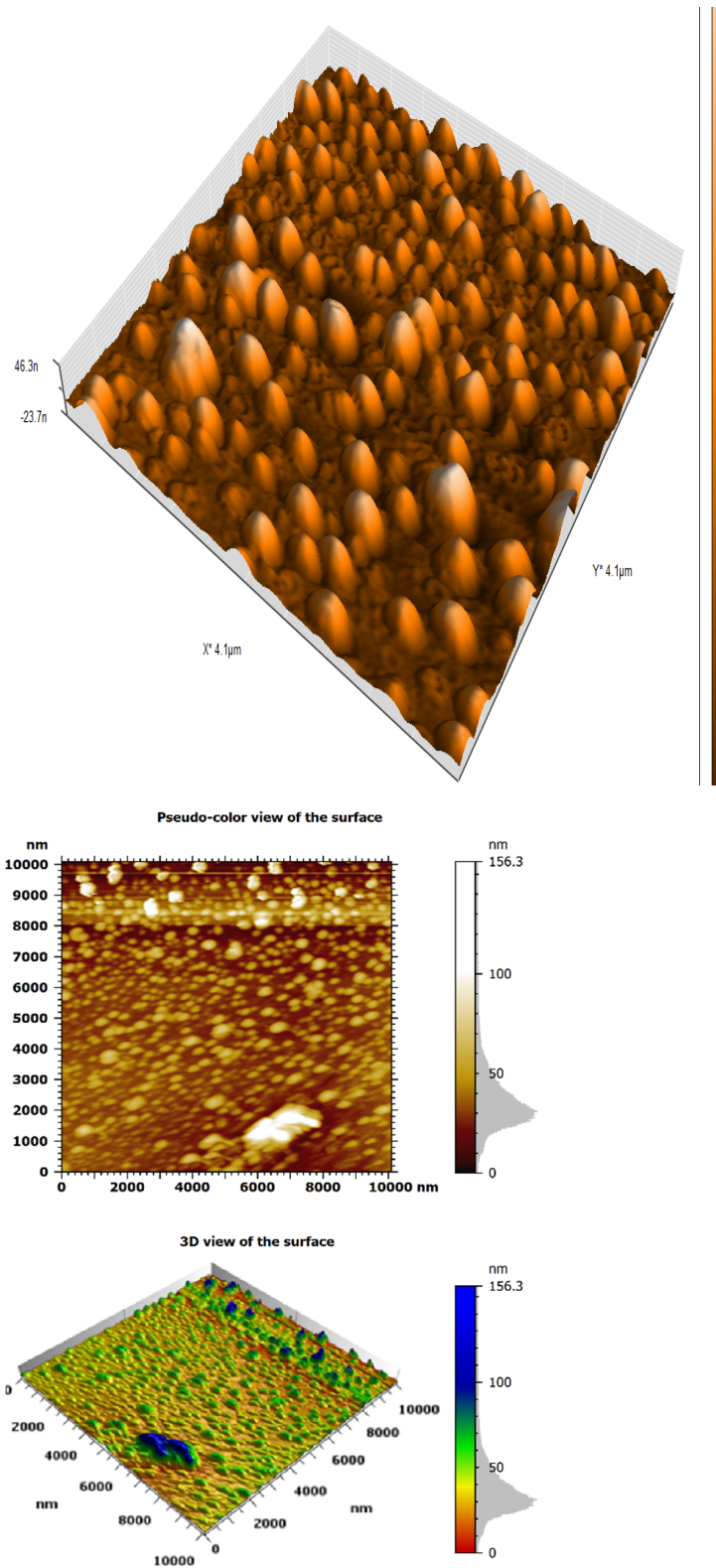


Fig. 4. The biosynthesized MgONPs under AFM, 2D and 3D images of MgONPs

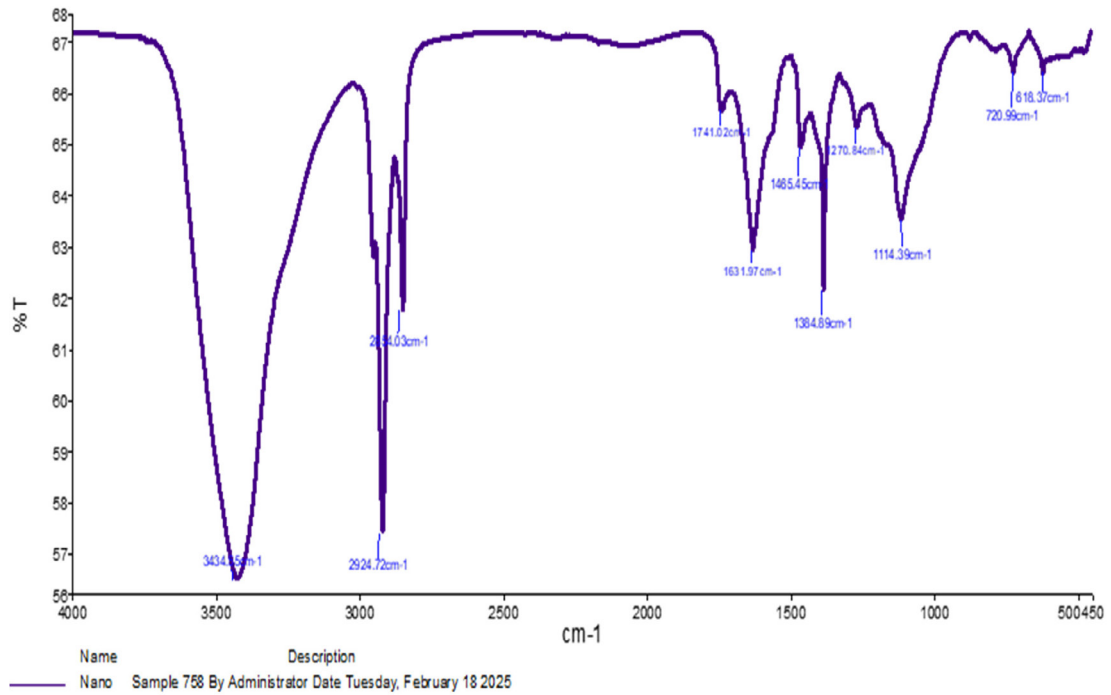


Fig. 4. FTIR spectra of MgONPs

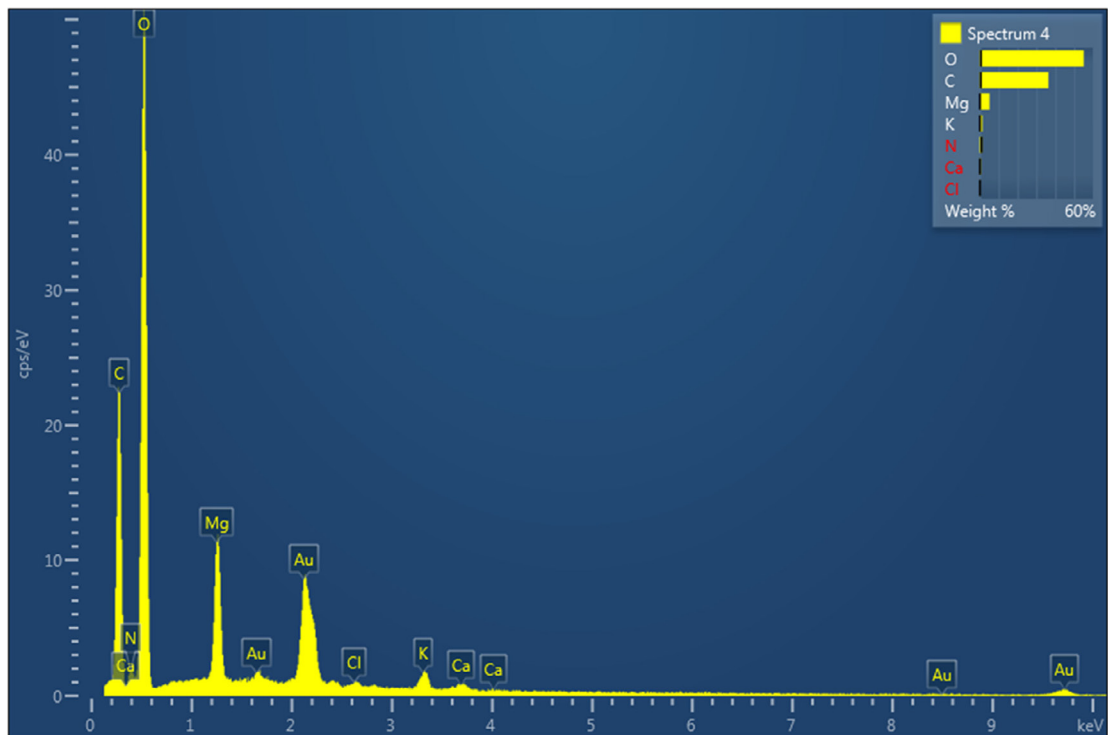
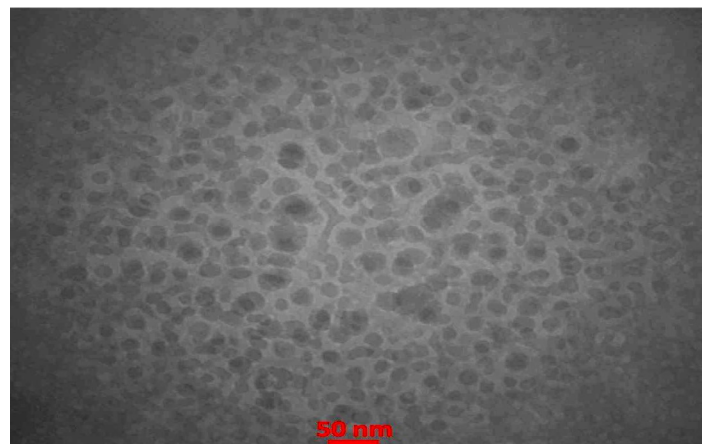


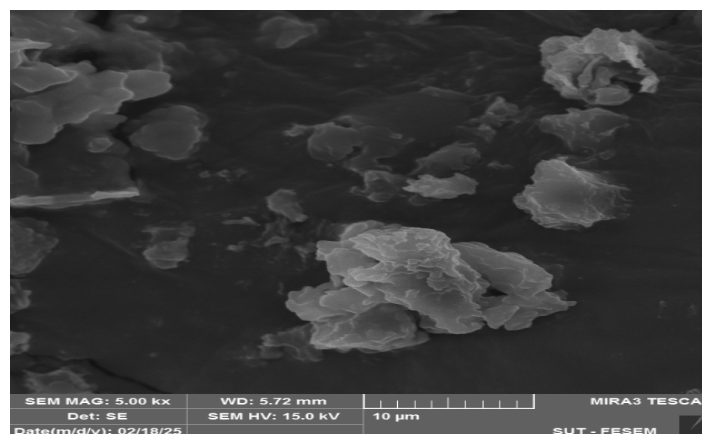
Fig. 5. The images of EDX analysis show Magnesium nanoparticles present with other elements.

Table 1. Energy dispersive X-ray (EDX) of MgONPs

Element	Line Type	Apparent Concentration	k Ratio	Wt%	Wt% Sigma	Atomic %	Standard Label	Factory Standard	Standard Calibration Date
C	K series	3.34	0.03339	36.33	0.54	44.30	C Vit	Yes	
N	K series	0.28	0.00049	1.27	0.92	1.32	BN	Yes	
O	K series	12.58	0.04234	55.17	0.65	50.50	SiO2	Yes	
Mg	K series	1.21	0.00804	5.08	0.10	3.06	MgO	Yes	
Cl	K series	0.07	0.00059	0.28	0.05	0.12	NaCl	Yes	
K	K series	0.35	0.00292	1.35	0.07	0.50	KBr	Yes	
Ca	K series	0.13	0.00115	0.52	0.07	0.19	Wollastonite	Yes	
Total:				100.00		100.00			



(a)



(b)

Fig.6. (a) TEM image bar 100 nm (b) SEM image, of MgONPs on 5kx bar 10 μm

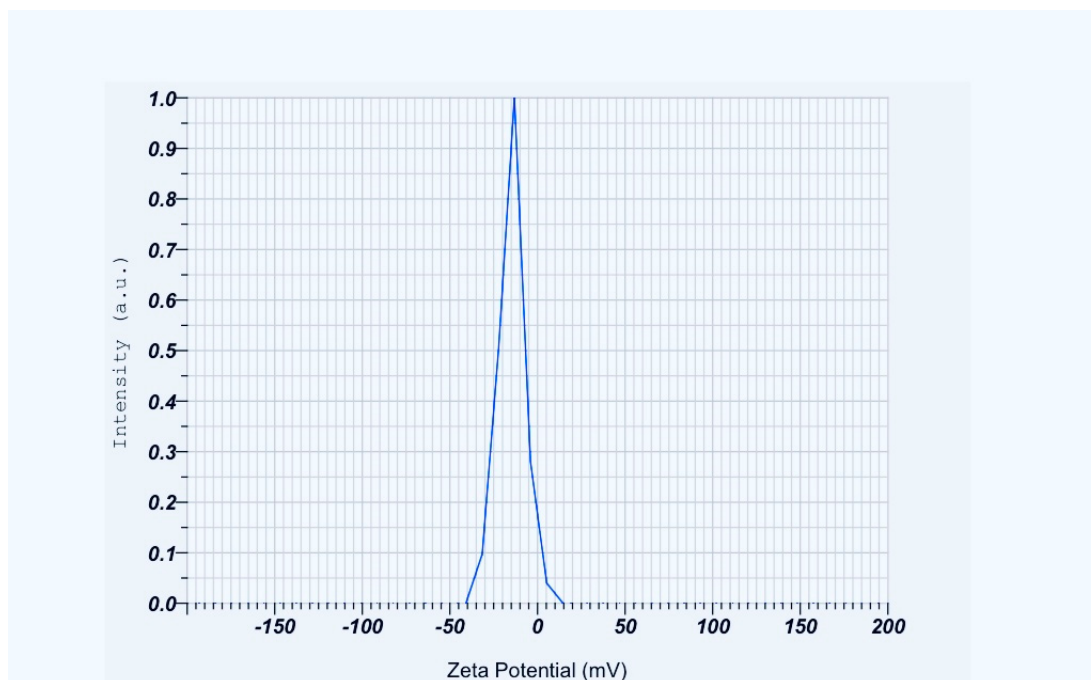


Fig. 7. Zeta potential of the synthesized MgONPs

of aggregation during drying or synthesis. A measurement of -20.1 mV for the zeta potential (Fig. 7) indicates considerable colloidal stability. Due to enough electrostatic repulsion, nanoparticles having zeta potentials more than -30 mV or greater than $+30$ mV are often regarded as extremely stable. In contrast, earlier research found that MgONPs made using pomegranate peel extract had smaller particle sizes, ranging from 42.4 to 57.7 nm, and a greater zeta potential of -68.93 mV, indicating improved stability and a more uniform dispersion.

The cytotoxic effect of MgONPs nanoparticles on tumor cell lines

The vast vascular network and its holes enable the transport of nutrients and oxygen to tumor tissues, as well as the accumulation and penetration of nanoparticles in these regions. As seen in Fig. 8, the cytotoxic effects of magnesium oxide nanoparticles (MgONPs) on the human breast cancer cell line MCF7 were assessed. When compared to untreated control cells, cells treated with MgONPs at doses of 50 $\mu\text{g/mL}$ and 100 $\mu\text{g/mL}$ showed morphological alterations.

As the concentration of MgONP increased, cell viability declined in a dose-dependent way. For

MgONPs, the dose needed to block 50% of MCF7 cell growth was around 11 $\mu\text{g/mL}$, as shown by the GI^{21} (Growth Inhibition 50%) value. MgONPs caused 65.4% cytotoxicity in MCF7 cells at a dose of 25 $\mu\text{g/mL}$. Cell viability consistently decreased with increasing nanoparticle concentrations when in vitro cytotoxicity was evaluated over a range of 6.25 – 100 $\mu\text{g/mL}$ (Fig. 9). These findings are in accordance with earlier research on a variety of cell lines and validate the cytotoxic capability of MgONPs at varied doses.

cytotoxicity results by offering more quantitative information (dose-dependent effects, % cytotoxicity at various dosages, and GI^{21} value). Additionally, we have explained the morphological alterations seen in MCF7 cells following MgONP treatment and provided comparisons with untreated control cells. The Results section now includes these changes (Figures 8 and 9). Additionally, we have bolstered our explanation whenever feasible by citing earlier research that corroborates our findings.

DISCUSSION

The results verify the effective synthesis of magnesium oxide nanoparticles (MgO-NPs) from *P. granatum* (pomegranate) peel aqueous extract. The extract's phytochemicals made it easier for

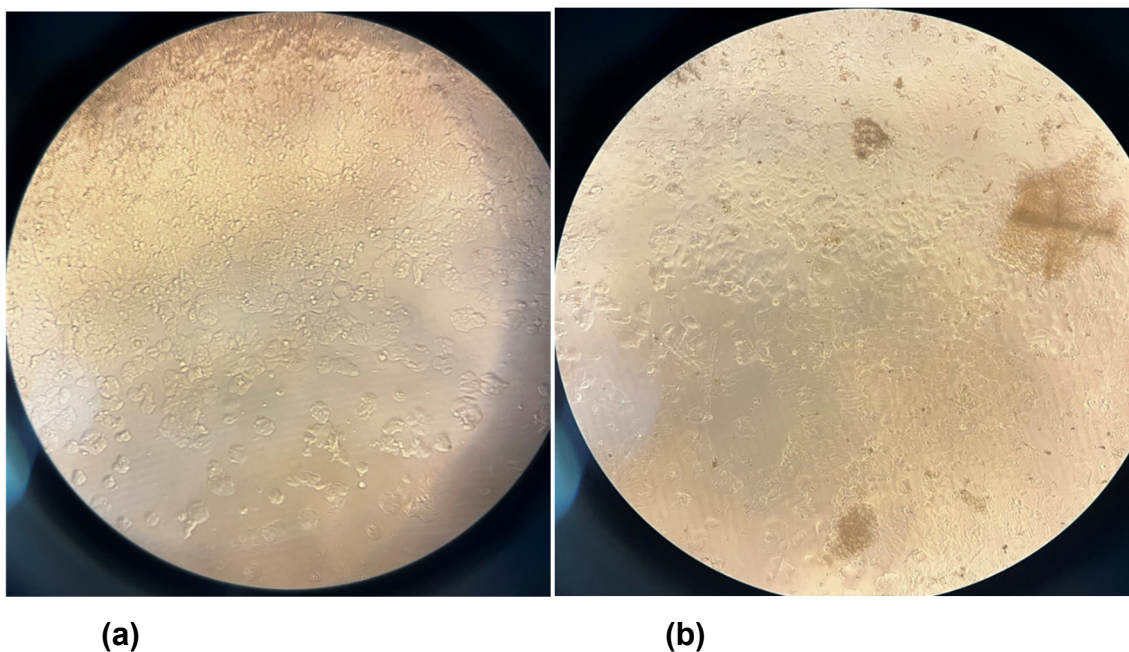


Fig. 8. The cytotoxic effect of MgONPs (a) Control MCF7 cells (b) MCF7 cells After treatment MgONPs at concentration 200 µg/ml at 200× magnification

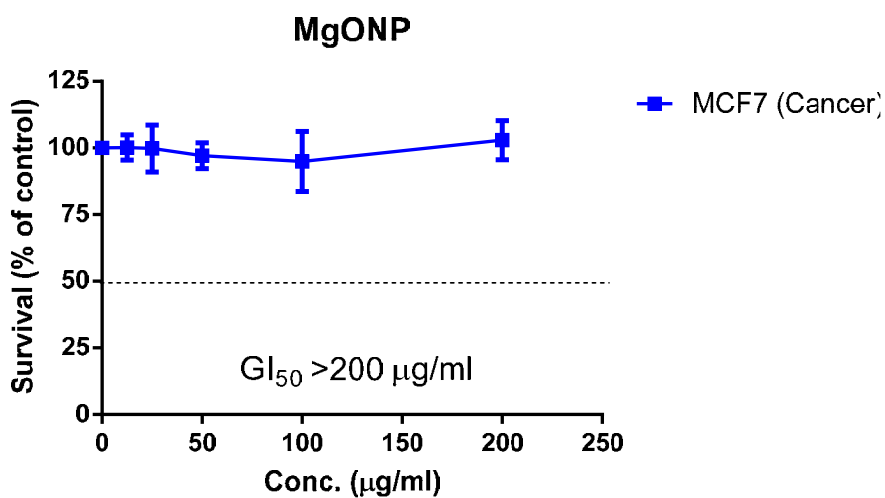


Fig. 9. The cytotoxic effect of MgONPs on MCF7 cells

magnesium ions to be reduced and stabilized into nanoscale oxide particles. Pomegranate peel contains a variety of compounds that are known to have important roles in the formation of nanoparticles by acting as natural reducing and capping agents, including flavonoids, phenolics, alkaloids, tannins, saponins, terpenoids, and steroids [16].

Through a variety of processes, including the

production of reactive oxygen species (ROS) such as hydrogen peroxide (H_2O_2), hydroxyl radicals ($\bullet OH$), and superoxide anions (O_2^-), as well as disruption of the microbial cell membrane, MgONPs have antibacterial action. These ROS cause oxidative stress, which damages essential cellular constituents including DNA, lipids, proteins, and amino acids and eventually causes microbial cell death. The microbial cell wall's structure also

affects how effective MgO-NPs are against bacteria. Gram-negative bacteria, which have a weaker cell wall, are often more vulnerable to MgO-NPs, whereas Gram-positive bacteria, with their thicker peptidoglycan layer, function as a physical barrier that can lessen nanoparticle penetration [17].

A number of factors, such as pH, plant extract concentration, and metal precursor concentration, were methodically assessed depending on the degree of color change in order to maximize the biosynthesis of MgO-NPs. The results showed that the most noticeable color shift, indicating ideal nanoparticle synthesis, was achieved by an alkaline pH of 8, a metal precursor concentration of 2 mM, and a plant extract ratio of 1:9 (1 mL plant extract: 9 mL deionized water containing the metal precursor). It has previously been established that the optimal pH for ecologically friendly MgO-NP synthesis is [18].

The ecological effects of MgO-NPs should be taken into account in addition to synthesis. For nourishment, certain mosquito larvae depend on particular microbes like bacteria and microalgae. MgO-NPs can suppress these microbial populations because of their antibacterial qualities, which may upset the food chain and have a negative impact on larval growth and survival. Particle size, concentration, length of exposure, and the kind of mosquito targeted all have an impact on the mosquitocidal effects of MgO-NPs [19].

Due to variations in their biological milieu, cancer cells are more vulnerable to nanoparticles than healthy cells. MgONPs have the ability to stop the cancer cell cycle, prevent cell division, and interfere with mitochondrial action, which can result in membrane potential loss and cell death. The goal of current research is to optimize MgONPs' therapeutic potential since these processes make them an attractive option for cancer treatment. In this work, we used HUFPP extract as a biological agent to biosynthesize iron oxide (FeO₃) and magnesium oxide (MgO) nanoparticles [20]. A dose-dependent MTT test was used to assess these nanoparticles' anticancer impact on HeLa cells.

HeLa cell viability and nanoparticle concentration were shown to be clearly correlated; as NP concentration rose, cell viability declined, indicating strong cytotoxic action [21]. Images using transmission electron microscopy (TEM) showed the size distribution and shape of the produced nanoparticles. The MgONPs measured between 14 and 20 nm, whereas the Fe₂O₃NPs

showed particle sizes between roughly 6 and 14 nm (Fig. 6) [22]. The effective biosynthesis of nanoparticles with sizes appropriate for biological purposes is confirmed by these results.

CONCLUSION

Magnesium oxide nanoparticles (MgONPs) have important antioxidant and anticancer properties and are used in dietary supplements. Numerous toxicity studies have shown that MgONPs are generally safe when taken at the prescribed doses. Future research should focus on creating characterization techniques, exploring the potential of MgONPs in targeted drug delivery systems, and improving green synthesis procedures in order to ensure scalability and environmental sustainability. MgONPs are useful nanomaterials with a wide range of biological uses. The biocompatibility and bioactivity of MgONPs produced using environmentally friendly, green methods have raised interest in their use. MgONPs were created in the current study using an easy, affordable, and ecologically friendly process.

- The resultant plant-derived MgONPs' physicochemical properties were examined using EDX, UV-Vis spectroscopy, TEM, AFM, DLS, and TGA-DTA methods. A number of variables, including as concentration, particle size and shape, surface charge, length of exposure, and level of cellular absorption, affect how poisonous MgONPs are. Chemical adsorption, electrostatic attraction, hydrophobic interactions, and chemical bonding are some of the ways that nanoparticles interact with cells.

ACKNOWLEDGEMENTS

The authors would like to acknowledge the Departments of Biology, College of Science, University of Baghdad and Medical and Molecular Biotechnology Department, Biotechnology Research Centre, Al-Nahrain University, for their great support in performing this work in their laboratories.

FUNDING SOURCES

The author(s) received no financial support for the research, authorship, and/or publication of this article.

CONFLICT OF INTEREST

The author(s) do not have any conflict of interest.

DATA AVAILABILITY STATEMENT

This statement does not apply to this article.

INFORMED CONSENT STATEMENT

This study did not involve human participants, and therefore, informed consent was not required.

CLINICAL TRIAL REGISTRATION

This research does not involve any clinical trials

AUTHOR CONTRIBUTION

Ameena Abdullah Rustum, and Adawia Fadhil Abbas writing original draft methodology, investigation, and formal analysis. Mais. Emad. The main concepts, data interpretation, supervision, and all were reviewed in the manuscript

REFERENCES

1. Hashem AH, AlAbboud MA, Alawlaqi MM, Abdelghany TM, Hasanin M. Synthesis of Nanocapsules Based on Biosynthesized Nickel Nanoparticles and Potato Starch: Antimicrobial, Antioxidant, and Anticancer Activity. *Starch-Stärke*. 2021;74(1-2):2100165. <https://doi.org/10.1002/star.202100165>
2. Ammulu MA, Viswanath KV, Giduturi AK, Vemuri PK, Mangamuri U, Poda S. Phytoassisted synthesis of magnesium oxide nanoparticles from *Pterocarpus marsupium* rox. b heartwood extract and its biomedical applications. *J Genet Eng Biotechnol*. 2021;19(1):21. <https://doi.org/10.1186/s43141-021-00119-0>
3. Ahmed ME, Sulaiman GM, Hasoon BA, Khan RA, Mohammed HA. Green Synthesis and Characterization of Apple Peel-Derived Selenium Nanoparticles for Anti-Fungal Activity and Effects of MexA Gene Expression on Efflux Pumps in *Acinetobacter baumannii*. *Appl Organomet Chem*. 2024;e7805. <https://doi.org/10.1002/aoc.7805>
4. Al-Rajhi AMH, Salem SS, Alharbi AA, Abdelghany TM. Ecofriendly synthesis of silver nanoparticles using Kei-apple (*Dovyalis caffra*) fruit and their efficacy against cancer cells and clinical pathogenic microorganisms. *Arab J Chem*. 2022;15(7):103927. <https://doi.org/10.1016/j.arabjc.2022.103927>
5. Elkodous MA, El-Husseiny HM, El-Sayyad GS, El-Sayyad AH, Doghish AS, Elfadil D, et al. Recent advances in waste-recycled nanomaterials for biomedical applications: Waste-to-wealth. *Nanotechnol Rev*. 2021;10(1):1662-739. <https://doi.org/10.1515/ntrev-2021-0099>
6. Dahee RJ, Ahmed ME, Hamid MK. Biogenic Selenium Nanoparticles via *Ralstonia Mannitolilytica*: Antimicrobial Activity and Expression of the MexA Gene of *Acinetobacter Bumannii*. *J Nanostruct*. 2025;15(1):310-25.
7. Rotti RB, Sunitha DV, Manjunath R, Roy A, Mayegowda SB, Gnanaprakash AP, et al. Green synthesis of MgO nanoparticles and its antibacterial properties. *Front Chem*. 2023;11:1143614. <https://doi.org/10.3389/fchem.2023.1143614>
8. Ahmed ME, Saleh IA, Al-Masri HA, Hamoud YA, Okla MK, Shaghaleh H. Green Synthesis of Copper Nanoparticles from Kiwi Peel: Antibacterial Properties and the Role of MexY Gene Expression in *Pseudomonas aeruginosa* Efflux Pumps. *Appl Biochem Biotechnol*. 2025;1-24. <https://doi.org/10.1007/s12010-025-05354-6>
9. Naseem K, Mir K, Sembiring KC, Khalid A, Khan ME, Deepati AK. Mango Peel Bio-actives for the Fabrication of Inorganic Metal Nanoparticles and their Potential for Wastewater treatment. *Water Air Soil Pollut*. 2025;236(2):1-18. <https://doi.org/10.1007/s11270-024-07728-8>
10. Khan MR, Alafaleq NO, Ramu AK, Alhosaini K, Khan MS, Zughaihi TA, et al. Evaluation of biogenically synthesized MgO NPs anticancer activity against breast cancer cells. *Saudi J Biol Sci*. 2024;31(1):103874. <https://doi.org/10.1016/j.sjbs.2023.103874>
11. Abdul Majeed SM, Ahmed ME, Hussein RH. Biogenic Synthesis and Characterization of Mango Peel-derived Selenium Nanoparticles for its Anti-Bacterial Potential. *J Nanostruct*. 2024;14(4):1347-57.
12. Fouda A, Alshallash KS, Alghonaim MI, Eid AM, Alemam AM, Awad MA, et al. The Antimicrobial and Mosquitocidal Activity of Green Magnesium Oxide Nanoparticles Synthesized by an Aqueous Peel Extract of *Punica granatum*. *Chemistry*. 2023;5(3):2009-24. <https://doi.org/10.3390/chemistry5030136>
13. Ahmed ME, Alzahrani KK, Fahmy NM, Almutairi HH, Almansour ZH, Alam MW. Colistin-Conjugated Selenium Nanoparticles: A Dual-Action Strategy Against Drug-Resistant Infections and Cancer. *Pharmaceutics*. 2025;17(5):556. <https://doi.org/10.3390/pharmaceutics17050556>
14. Fadhil AA, Ahmed ME. Characterization of chitosan-based copper nanoparticles: Synthesis approach, antimicrobial activity, and cytotoxicity assay investigation. *Microb Biosyst*. 2025;10(2):[Article in Press]. <https://doi.org/10.21608/mb.2025.355421.1238>
15. Ahmed ME, Hamza Faiq N, Almutairi HH, Alam MW. Biosynthesized ZnO-CuO Nanocomposite for Biofilm Formation of *Proteus mirabilis* upon LuxS Gene Expression. *Inorganics*. 2025;13(2):65. <https://doi.org/10.3390/inorganics13020065>
16. Hassan SE, Fouda A, Saied E, Farag MMS, Eid AM, Barghoth MG, et al. Rhizopus oryzae-Mediated Green Synthesis of Magnesium Oxide Nanoparticles (MgO-NPs): A Promising Tool for Antimicrobial, Mosquitocidal Action, and Tanning Effluent Treatment. *J Fungi (Basel)*. 2021;7(5):372. <https://doi.org/10.3390/jof7050372>
17. Tamam N, Mahadadalkar MA, Aadil M, El-Aassar MR, Rafea MA, Zaki ME, et al. Unveiling the visible-light-driven photocatalytic aptitude of nanostructured MgO semiconductor synthesized using lemon peel extract. *Ceram Int*. 2025;[Article in Press]. <https://doi.org/10.1016/j.ceramint.2025.03.231>
18. Fouda A, Awad MA, Eid AM, Saied E, Barghoth MG, Hamza ME, et al. An Eco-Friendly Approach to the Control of Pathogenic Microbes and *Anopheles stephensi* Malarial Vector Using Magnesium Oxide Nanoparticles (Mg-NPs) Fabricated by *Penicillium chrysogenum*. *Int J Mol Sci*. 2021;22(10):5096. <https://doi.org/10.3390/ijms22105096>
19. Ahmed ME, Al-Awadi AQ, Abbas AF. Focus of Synergistic Bacteriocin-Nanoparticles Enhancing Antimicrobial Activity Assay. *Microbiol J*. 2023;85(6):95-104. <https://doi.org/10.15407/microbiolj85.06.095>
20. Daniele V, Volpe AR, Cesare P, Taglieri G. MgO

- Nanoparticles Obtained from an Innovative and Sustainable Route and Their Applications in Cancer Therapy. *Nanomaterials (Basel)*. 2023;13(22):2975. <https://doi.org/10.3390/nano13222975>
21. Amina M, Al Musayeb NM, Alarfaj NA, El-Tohamy MF, Oraby HF, Al Hamoud GA, et al. Biogenic green synthesis of MgO nanoparticles using *Saussurea costus* biomasses for a comprehensive detection of their antimicrobial, cytotoxicity against MCF-7 breast cancer cells and photocatalysis potentials. *PLoS One*. 2020;15(8):e0237567. <https://doi.org/10.1371/journal.pone.0237567>
22. Oyshi SA, Jahan RA, Aktar F, Sultan MZ, Chowdhury AA, Chowdhury JA, et al. Preparation and evaluation of the biosynthetic procedure of iron oxide and magnesium oxide nanoparticles using *Hylocereus undatus* fruit peel extract and their anticancer properties. *RSC Adv*. 2025;15(19):15366-74. <https://doi.org/10.1039/D4RA07411D>